Investigation of particles size effects in Dissipative Particle Dynamics (DPD) modelling of colloidal suspensions

N. Mai-Duy[1,2], N. Phan-Thien[1,*] and B.C. Khoo[1]
[1] Department of Mechanical Engineering, Faculty of Engineering,
National University of Singapore, Singapore.
[2]Computational Engineering and Science Research Centre,
School of Mechanical and Electrical Engineering,
University of Southern Queensland, Toowoomba, QLD 4350, Australia.

Submitted to *Computer Physics Communications*, April 2014; revised (1), November 2014; revised (2), December 2014

Abstract In the Dissipative Particle Dynamics (DPD) simulation of suspension, the fluid (solvent) and colloidal particles are replaced by a set of DPD particles and therefore their relative sizes (as measured by their exclusion zones) can affect the maximal packing fraction of the colloidal particles. In this study, we investigate roles of the conservative, dissipative and random forces in this relative size ratio (colloidal/solvent). We propose a mechanism of adjusting the DPD parameters to properly model the solvent phase (the solvent here is supposed to have the same isothermal compressibility to that of water).

Keywords: Dissipative particle dynamics, colloidal suspensions, volume packing fraction, solvent particle size, spring model

1 Introduction

Particulate suspensions, fluids with suspended rigid particles, occur in many industrial processes [1]. If the sizes of the suspended particles are in the range of nanometers to micrometers, the micromechanics problems are said to be on a mesoscopic length scale. Effective numerical methods

*Corresponding author: E-mail nhan@nus.edu.sg, Telephone +65-6601-2054, Fax +65-6779-1459

dealing with these problems can be classified into two groups. In the first group, it is recognised that suspended particles inertia is insignificant (corresponding to zero Reynolds number), and their behaviour is governed by the linearised Stokes equations. Stokes analytic solutions for one and two interacting spheres are available, from which one can construct a grand resistance matrix for a generic particle, which relates the force/torque exerted by the fluid on it to the particle's velocities, which can be solved for the motion of the particle concerned. This is the basis for Stokesian Dynamics (SD) [2]. An accelerated version of SD, which requires only $O(N \log N)$ operations (N is the number of spheres), has been proposed [3]; however, SD methods encounter challenges in modelling particles of arbitrary shape, or in non-zero particle Reynolds number, or in a non-Newtonian suspending liquid. In the second group, the suspending liquid is modelled explicitly by particles. Hydrodynamic interactions are taken into account by solving the full set of hydrodynamic equations, and thus some of the difficulties associated with SD are eliminated. This group includes the lattice Boltzmann methods [4], dissipative particles dynamics (DPD) [5], smooth dissipative particles dynamics (sDPD) [6]. sDPD is a particle-based solution method, where the formulation for simulation is derived from the direct discretisation of the Navier-Stokes equation (macroscopic/continuum mechanics equation) with the inclusion of thermal fluctuations. Strengths of dissipative and random forces are related via a fluctuation-dissipation theorem. An sDPD solution to a mesoscopic problem is thus constructed from the top-down approach (from the Navier-Stokes to the particles motion equations). On the other hand, DPD, originally designed for the simulation of complex fluids on mesoscopic length scale, is a bottom-up approach (from the particles to the Navier-Stokes equations). The method is based on molecular dynamics to construct a solution to a mesoscopic problem. In the method, the fluid and everything in it are replaced with particles (called DPD particles), each particle not only contains a cluster of fluid particles, but also in some sense represents a position and momentum of a region of the fluid [7]. The forces acting on particles are pairwise, centre-to-centre and zero outside a cutoff radius. The resultant mean velocities and stresses have been shown to satisfy the Navier-Stokes equations. Advantages of DPD over other mesoscopic methods lie in its simplicity in modelling multiphase complex structure fluids. Each phase can be modelled by a set of DPD particles with appropriate forms of interactions. It is noted that the DPD method does not require *a-priori* constitutive knowledge of the fluid. The constitutive framework is fully specified in the microstructure that goes into the description of the DPD model (the relevant constitutive law will result from the fluid

description) [8].

In this paper, we are concerned with the DPD modelling of particulate suspensions, where the solvent phase is replaced by a system of DPD particles, referred to here as "solvent particles". The suspended phase has been modelled with either the single particle models [9,10,11,12,13] or the frozen particle models [14,15,16]. Recently, a new suspended-particle model has been proposed using just a few basic DPD particles (referred to here as "constituent particles") connected to reference sites by stiff linear springs [17]; the reference sites move as a rigid body motion. Compared to the single DPD particle models, the spring model works well with larger time steps (only soft potentials are employed here), involves considerably less parameters (the dispersion phase is also based on basic DPD particles and consequently, the solvent-colloidal interaction can be decomposed into a set of solvent-solvent interactions), and can be extended to the case of suspended particles of non-spherical/-circular shapes more straightforwardly. It was reported in [17] that the single particle model employs a time step in the range of 0.0002 to 0.0005. The time steps used in the spring model are 0.005-0.01 for 2D and 0.001-0.005 for 3D (i.e., about one order of magnitude higher). Using the spring model, the simulations of particulate suspensions only involve DPD parameters of the fluid case and one extra parameter, namely the stiffness of springs, which can be easily chosen. Compared to the frozen particle models, the spring model employs only a few DPD particles to represent a suspended particle (we found that the size of a colloidal particle is actually defined by the repulsive force field generated by constituent particles of that particle (not by their locations on the surface)). With the spring model, one can employ only 4 and 8 basic DPD particles to model a suspended cylinder and sphere, respectively. Furthermore, the solvent particles and the constituent particles (on a suspended particle) follow the same types of interactions, with the same values of the DPD parameters. This allows a simple but effective implementation, and allows a particle volume fraction to be defined, which then recovers the celebrated Einstein's relation for the effective viscosity at low volume fractions.

For the modelling of single phase systems, DPD is known to possess a scale-free property over the whole mesoscopic range [18]. The larger the number of fluid molecules packed into a DPD particle (larger DPD particle), the higher the coarse graining level will be. With an appropriate scaling scheme, numerical results from solving the DPD equations of motion can be independent to the number density chosen. Such a scaling scheme, requiring one single length scale, is no longer valid

in the simulation of particulate suspensions, where there are more than one length scale. The size of the suspended particles in colloidal suspensions is in the range of nanometers to micrometers. If the DPD system representing the solvent is employed on a coarse graining level approaching the suspended particle size, there will be an influence on the maximal packing fraction of the colloids and thus on the suspension rheology, especially in the concentrated regime. These effects were reported in [17], where the DPD system considered has a variable isothermal compressibility and reducing the temperature is shown to strongly affect the size ratio of the colloidal to solvent particles.

The present work will investigate in detail the effect of the solvent particle size in the DPD systems whose isothermal compressibility is matched with that of water at room temperature, and also further verify the spring model with a larger number of constituent particles than has been hitherto used. Roles of the DPD forces in making the particles' exclusion zones are analysed throughout for the first time. It will be shown that the Boltzmann temperature has a completely different effect on the bulk material properties between the two cases: variable and fixed compressibility. The case of variable compressibility has been considered in [17]. A simple mechanism of choosing the DPD parameters to effectively control the solvent particle size is proposed and verified.

The paper is organised as follows. Brief reviews of the DPD method and spring model for suspended particles are given in Sections 2 and 3, respectively. Effects of solvent particles size are discussed in Section 4. Numerical results are presented in Section 5. Section 6 gives some concluding remarks.

2 Dissipative particle dynamics (DPD)

In the DPD method, the fluid is replaced by a system of DPD particles undergoing their Newtonian 2nd law motion:

$$m_i \ddot{\mathbf{r}}_i = m_i \dot{\mathbf{v}}_i = \sum_{j=1, j\neq i}^{N} \left(\mathbf{F}_{ij,C} + \mathbf{F}_{ij,D} + \mathbf{F}_{ij,R} \right), \tag{1}$$

where m_i, $\mathbf{r}_i$ and $\mathbf{v}_i$ represent the mass, position vector and velocity vector of a particle $i = 1, \ldots, N$, respectively, N is the total number of DPD particles, the superposed dot denotes a time derivative, and the three forces on the right side of (1) represent a conservative force (subscript C) that can be utilised to control the speed of sound independently of the temperature and density of the DPD

system, a dissipative force (subscript D) proportional to the relative velocity of particle j to i, and a random force (subscript R) modelled by white noise

$$\mathbf{F}_{ij,C} = a_{ij} w_C \mathbf{e}_{ij}, \tag{2}$$

$$\mathbf{F}_{ij,D} = -\gamma w_D \left(\mathbf{e}_{ij} \cdot \mathbf{v}_{ij}\right) \mathbf{e}_{ij}, \tag{3}$$

$$\mathbf{F}_{ij,R} = \sigma w_R \theta_{ij} \mathbf{e}_{ij}, \tag{4}$$

where a_{ij}, γ and σ are constants reflecting the strengths of these forces, w_C, w_D and w_R the configuration-dependent weighting functions to be defined below, $\mathbf{e}_{ij} = \mathbf{r}_{ij}/r_{ij}$ a unit vector from particle j to particle i ($\mathbf{r}_{ij} = \mathbf{r}_i - \mathbf{r}_j$, $r_{ij} = |\mathbf{r}_{ij}|$), $\mathbf{v}_{ij} = \mathbf{v}_i - \mathbf{v}_j$ the relative velocity vector, and θ_{ij} a Gaussian white noise ($\theta_{ij} = \theta_{ji}$) with stochastic properties

$$\langle \theta_{ij} \rangle = 0, \tag{5}$$

$$\langle \theta_{ij}(t) \theta_{kl}(t') \rangle = \left(\delta_{ik}\delta_{jl} + \delta_{il}\delta_{jk}\right) \delta\left(t - t'\right), \tag{6}$$

in which $\delta(t - t')$ is the Dirac delta function, and δ_{ij} the Kronecker delta.

All these interaction forces are pairwise, center-to-center, and zero outside a cutoff radius. The dissipative force cannot be chosen independently to the random force, if the specific energy of the system (Boltzmann temperature $k_B T$) is to be maintained. This is the essence of the fluctuation-dissipation theorem [19]

$$w_D(r_{ij}) = \left(w_R(r_{ij})\right)^2, \tag{7}$$

$$k_B T = \frac{\sigma^2}{2\gamma}. \tag{8}$$

A popular choice of the weighting functions is [20,21]

$$w_C(r_{ij}) = 1 - \frac{r_{ij}}{r_c}, \tag{9}$$

$$w_D(r_{ij}) = \left(1 - \frac{r_{ij}}{r_c}\right)^s. \tag{10}$$

where s is a constant ($s = 2$ and $s = 1/2$ are two typical values of s). $s = 1/2$ is adopted in this study.

We may re-write the stochastic DPD equation (1) in the following differential form

$$\Delta \mathbf{v}_i = \frac{1}{m_i} \sum_{j \neq i} a_{ij} w_C \Delta t \mathbf{e}_{ij} - \frac{1}{m_i} \sum_{j \neq i} \gamma w_D \left(\mathbf{e}_{ij} \cdot \mathbf{v}_{ij} \right) \Delta t \mathbf{e}_{ij} + \frac{1}{m_i} \sum_{j \neq i} \sigma w_R \Delta W_{ij}(t, \Delta t) \mathbf{e}_{ij}, \tag{11}$$

where

$$\Delta W_{ij}(t, \Delta t) = \int_t^{t+\Delta t} \theta_{ij}(s) ds. \tag{12}$$

The incremental stochastic process ΔW_{ij} has zero mean and autocorrelation

$$\langle \Delta W_{ij}(\Delta t) \Delta W_{kl}(\Delta t) \rangle = \left(\delta_{ik} \delta_{jl} + \delta_{il} \delta_{jk} \right) \Delta t. \tag{13}$$

If we define $\Delta W_{ij} = \xi_{ij} \sqrt{\Delta t}$, then ξ_{ij} is a random tensor with zero mean and variance $\langle \xi_{ij} \xi_{kl} \rangle = (\delta_{ik}\delta_{jl} + \delta_{il}\delta_{jk})$. This random tensor can be chosen from a pseudo-random sequence, and (11) is the basis for updating a particle velocity. Since w_C, w_D and w_R are dimensionless functions, the DPD parameters a_{ij}, γ, σ and $k_B T$ have units of $[F]$, $[FT/L]$, $[F\sqrt{T}]$ and $[FL]$, respectively, where $[F]$ is the force unit, $[T]$ is the unit of time, $[L]$ is the unit of length.

For a given domain of interest, different number densities of particles (different coarse graining levels) can be employed to represent the fluid in the domain [18]. As the number density is reduced, one has a higher coarse-graining level and a larger particles size. The level of coarse graining level may be identified with the number density. With an appropriate scaling scheme, similar results from solving the DPD equations of motion can be obtained for any values of the particle number density (scale-free property, [18]).

After tracking the state of the system (positions and velocities), we can define the density and the linear momentum of the fluid as

$$\rho(\mathbf{r}, t) = \sum_i \langle m_i \delta(\mathbf{r} - \mathbf{r}_i) \rangle, \quad \rho(\mathbf{r}, t) \mathbf{u}(\mathbf{r}, t) = \sum_i \langle m_i \dot{\mathbf{r}}_i \delta(\mathbf{r} - \mathbf{r}_i) \rangle, \tag{14}$$

and it can be shown [22,7] that

$$\frac{\partial}{\partial t} \rho + \nabla \cdot (\rho \mathbf{u}) = 0, \qquad \nabla = \partial / \partial \mathbf{r}, \tag{15}$$

$$\frac{\partial}{\partial t} (\rho \mathbf{u}) + \nabla \cdot (\rho \mathbf{u}\mathbf{u}) = \nabla \cdot \mathbf{T}, \tag{16}$$

which are recognised as the usual conservation laws - they are the consequence of the DPD particles mechanics (1). The stress tensor in (16) is given by [23]

$$\mathbf{T} = -\frac{1}{V}\left[\sum_i m\mathbf{V}_i\mathbf{V}_i + \frac{1}{2}\sum_i\sum_{j\neq i}\mathbf{r}_{ij}\mathbf{F}_{ij}\right] = -n\left(\langle m\mathbf{V}\mathbf{V}\rangle + \frac{1}{2}\langle\mathbf{r}\mathbf{F}\rangle\right), \tag{17}$$

where n is the number density of particles, V is the volume of the bin and $\mathbf{V}_i$ is the velocity fluctuation of particle i with respect to the mean field velocity (peculiar velocity), and the angular brackets denote an ensemble average. The first term on the right side of (17) denotes the contribution to the stress from the momentum (kinetic) transfer of DPD particles and the second term from the interparticle forces. Two important points should be noted: (i) the method is truly a particle-based method, in the sense that it guarantees the satisfaction of conservation laws; and (ii) the stress, as a result of the microstructure specification, can be posteriori determined from the system state.

3 Spring model for suspended particles

The rationale behind the spring model [17] is that the shape of a colloid is actually defined by the repulsion force field generated by constituent particles of that colloid. In the spring model, a colloidal particle is modelled by using only a few basic DPD particles that are connected to the reference sites (on that colloidal particle) by linear springs of very large stiffness (Figure 1). For example, a spherical particle can be simply represented using 6 or 8 basic DPD particles with their reference sites at the vertices of either an octahedron or a cube, respectively. The reference sites, collectively modelling a rigid body, move as a rigid body motion calculated through their

Newton-Euler equations, using data from the previous time step,

$$M_c^k \frac{d\mathbf{V}_c^k}{dt} = \mathbf{F}^k(t-\Delta t), \tag{18}$$

$$\mathbf{I}^k \frac{d\boldsymbol{\omega}^k}{dt} = \mathbf{T}^k(t-\Delta t), \tag{19}$$

$$\mathbf{F}^k(t-\Delta t) = \sum_{i=1}^{p} \sum_{j=1, j\neq i}^{N} \left[\mathbf{F}_{ij,C}^k(t-\Delta t) + \mathbf{F}_{ij,D}^k(t-\Delta t) + \mathbf{F}_{ij,R}^k(t-\Delta t)\right], \tag{20}$$

$$\mathbf{T}^k(t-\Delta t) = \sum_{i=1}^{p} \left(\mathbf{r}_i^k(t-\Delta t) - \mathbf{R}_c^k(t-\Delta t)\right) \times \sum_{j=1, j\neq i}^{N} \left[\mathbf{F}_{ij,C}^k(t-\Delta t) + \mathbf{F}_{ij,D}^k(t-\Delta t) + \mathbf{F}_{ij,R}^k(t-\Delta t)\right], \tag{21}$$

where M_c^k, $\mathbf{I}^k$, $\mathbf{R}_c^k$, $\mathbf{r}_i^k$, $\mathbf{V}_c^k$, $\boldsymbol{\omega}^k$ and p are the mass, moment of inertia tensor, centre of mass, position of particle i, centre-of-mass velocity, angular velocity, number of constituent particles of the kth colloidal particle, respectively.

The velocities of their associated DPD particles are found by solving the DPD equations at the current time step

$$\mathbf{F}_i^k(t) = \sum_{j=1, j\neq i}^{N} \left[\mathbf{F}_{ij,C}^k(t) + \mathbf{F}_{ij,D}^k(t) + \mathbf{F}_{ij,R}^k(t)\right] + \mathbf{F}_{i,S}^k(t), \quad i = (1, 2, \cdots, p). \tag{22}$$

where $\mathbf{F}_{i,S}^k(t) = -H\left[\mathbf{r}_i^k(t) - \overline{\mathbf{r}}_i^k(t)\right]$ is the spring force with H being the stiffness of the spring and $\overline{\mathbf{r}}_i$ the position of the reference site i. Introducing springs into the model allows the constituent particles to fully participate in the system dynamics, leading to a better control of the system temperature. The spring stiffness is chosen large to ensure a good representation of rigid particles, but not infinity to get some fluctuating motion. As in [17], $H = 3000$ (DPD units) is employed here. Note that in the stiff limit ($H \to \infty$), our proposed model exactly reduces to a frozen particle model. There are no time step constraints due to springs on equations being solved.

One distinguishing feature of the spring model is that the solvent particles and the constituent particles of the suspended particles use the same values of the DPD parameters including the Boltzmann temperature (contrasting to different sets of DPD parameters, solvent-solvent, solvent-colloidal, colloidal-colloidal, in one-single DPD particle models). Consequently, the resultant DPD system is based on identical basic particles, and the particle volume fraction can be simply defined

as

$$\phi = \frac{N_c^0}{N_c^0 + N_s}, \tag{23}$$

where N_c^0 and N_s are the numbers of the basic DPD particles used to represent the solvent and colloidal phases, respectively. Numerical results show that this definition of the volume fraction (23) (which is the number fraction) recovers Einstein's relation at low volume fraction irrespective of values of the input DPD parameters, and therefore is appropriate for DPD suspensions.

4 Investigation of effects of solvent particle size

In DPD, monodispersed suspensions are modelled through two sets of particles: one for the solvent phase (basic DPD particles freely movable) and the other for the dispersion phase (in the present work, by basic DPD particles that are constrained according to the spring model). The kinetic theory [7], confirmed by numerical results, shows that there is an exclusion zone associated with a basic DPD particle. The size of this exclusion zone may be sensibly defined as the particle size. This particle size can be assessed by means of the radial distribution function. Note that the cutoff radius does not necessarily represent the size of the DPD particle - a larger cutoff radius may result in a smaller size of the particle as will be shown later. The cutoff radius and the effective size are two different concepts. If the solvent particle size is significant (compared to colloidal size), the maximal packing fraction of the colloidal particles will be reduced. Consequently, the relative viscosity is expected to diverge earlier as the volume fraction increases approaching the maximal packing fraction, and the shear thinning behaviour becomes stronger. Controlling the solvent particle size to have a correct representation of the solvent phase (in the sense that the colloidal/solvent size ratio is very large) is a vital issue in the DPD modelling of colloidal suspensions. In what follows, we analyse roles of the DPD forces on the particle's exclusion size. Until noted, only a single phase system (solvent) is considered in the following discussions.

4.1 Role of the conservative force

The inclusion of the conservative force (repulsive force) into the DPD formulation is to provide an independent mean of controlling the speed of sound (compressibility) to the number density and the temperature of the DPD system [7]. Keeping the dissipative and random forces unchanged, an increase in the repulsion strength a_{ij} will promote incompressibility of the DPD fluid [24]. However, at large values of a_{ij}, the mean squared particle displacement $\left\langle (\mathbf{r}(t) - \mathbf{r}(0))^2 \right\rangle$ is observed to be no longer linear in time with crystallisation occuring and the DPD system has a solid-like structure. In the present work, we limit our attention to the case where the compressibility of the system is matched to that of the water at room temperature [20]. In [17], this constraint of constant compressibility was not enforced, and therefore comparison across different fluids must be taken carefully. The effects of the Boltzmann temperature k_BT on the maximum packing fraction of the colloidal particles and the degree of shear-thinning can be significant for the case of variable compressibility as shown in [17]. It will be shown here that the mentioned effects can be negligible for the case of fixed compressibility.

From the virial theorem [23], the pressure is computed as

$$p = nk_BT + \frac{n^2}{2d} \int d\mathbf{r} r F_{ij,C}(r) g(r), \tag{24}$$

where $g(r)$ is the radial distribution function and d the flow dimensionality. Here, we simply take $g(r) = 1$ corresponding to an infinite number of DPD particles.

Expression (24) results in

$$p = nk_BT + \frac{1}{2}\frac{n^2}{2} \int_0^{r_c} 2\pi r dr \left[r a_{ij} \left(1 - \frac{r}{r_c} \right) \right] = nk_BT + \frac{\pi}{24} a_{ij} n^2 r_c^3, \tag{25}$$

$$\frac{\partial p}{\partial n} = k_BT + \frac{\pi}{12} a_{ij} n r_c^3, \tag{26}$$

for 2D case, and

$$p = nk_BT + \frac{1}{2}\frac{n^2}{3} \int_0^{r_c} 4\pi r^2 dr \left[r a_{ij} \left(1 - \frac{r}{r_c} \right) \right] = nk_BT + \frac{\pi}{30} a_{ij} n^2 r_c^4, \tag{27}$$

$$\frac{\partial p}{\partial n} = k_BT + \frac{\pi}{15} a_{ij} n r_c^4, \tag{28}$$

for 3D case.

The isothermal compressibility can be represented through the following dimensionless parameter

$$\kappa^{-1} = \frac{1}{k_B T} \frac{\partial p}{\partial n}. \tag{29}$$

For water at room temperature, one has $\kappa^{-1} = 15.98$. Substitution of (26) and (28) into (29) yields, respectively,

$$a_{ij} = \frac{57.23 k_B T}{n r_c^3} \tag{30}$$

for 2D case, and

$$a_{ij} = \frac{71.54 k_B T}{n r_c^4} \tag{31}$$

for 3D case.

If the weighting function w_C is fixed at the linear form, as adopted in this work, the size of solvent particles induced by the conservative forces will be controlled by means of the repulsion parameter a_{ij}. A larger value of a_{ij} results in a larger size of the particle and vice versa. From expressions (30) and (31), one can reduce the particle size by increasing n, increasing r_c or reducing $k_B T$. These expressions also reveal that the larger the DPD particles size (corresponding to larger a_{ij}), the coarser level (smaller n) the DPD system will be (this comes from the scaling property of the DPD system [18]).

4.2 Role of the dissipative and random forces

Consider a generic "tagged" DPD particle in a sea of other DPD particles undergoing a diffusion process. Its size a_{eff} may be estimated by the Stokes-Einstein relation

$$a_{eff} = \frac{k_B T}{6\pi D \eta}, \tag{32}$$

where D is the diffusion coefficient of the tagged particle subject to Brownian motion in an unbounded domain and η the shear viscosity of the surrounding fluid.

In the absence of the conservative force ($\mathbf{F}_{ij,C} = 0$), using standard kinetic theory, the expressions

for the viscosity and diffusivity have been derived as [25]

$$\eta = \frac{3mk_BT}{2\gamma[w_D]_R} + \frac{\gamma n^2[R^2 w_D]_R}{30}, \tag{33}$$

$$D = \frac{3k_BT}{n\gamma[w_D]_R}, \tag{34}$$

where $[w_D]_R = \int d\mathbf{R} w_D(R)$ and $[R^2 w_D(R)] = \int d\mathbf{R} R^2 w_D(R)$.

In this study, we adopt the form $w_D(r)$ due to [21]

$$w_D(r) = \begin{cases} (1 - r/r_c)^{1/2}, & r < r_c \\ 0, & r \geq r_c \end{cases}, \tag{35}$$

and thus

$$D = \frac{315}{32\pi}\frac{(k_BT)^2}{\sigma^2 n r_c^3}, \tag{36}$$

$$\eta = \frac{315}{64\pi}\frac{m(k_BT)^2}{\sigma^2 r_c^3} + \frac{256\pi}{51975}\frac{\sigma^2 n^2 r_c^5}{k_BT}. \tag{37}$$

Substitution of (36) and (37) into (32) yields

$$a_{eff} = \frac{56320\pi n\sigma^4 r_c^6}{315 \times 51975 m(k_BT)^3 + 64 \times 256\pi^2\sigma^4 n^2 r_c^8}. \tag{38}$$

Note that expression (38) is established assuming the Stokes-Einstein relation, which is concerned with the dispersion of mesoscopic particles in a continuous solvent. The DPD particles representing the solvent phase are assumed not to be clustered, and are of a size considerably less than that of the tagged particle that has no inertia. This latter condition is of course not satisfied here and the expression (38) can only be considered as best an estimate. However, the solvent particle size approaches zero as any one of the number density n, the cutoff radius r_c and the thermodynamic temperature k_BT approaches infinity.

Although expression (38) is only an approximate result, but it serves as a mean to gauge the effect of different parameters. Figures 2, 3 and 4 show respectively the effects of n, r_c and k_BT on the solvent particle size. Figures 2 and 3 clearly indicate that the exclusion zones caused by the conservative force and by the dissipative and random forces are both smaller with increasing either n or r_c. However, in Figure 4, the solvent particle size is an increasing function of k_BT with

the conservative force, and a decreasing function of k_BT with the dissipative and random forces. Special care is thus needed if one tries to control the solvent particle size via k_BT. It is noted that (i) reducing k_BT makes a_{ij} smaller which can result in the clustering of particles; and (ii) the particle size, defined in (38), is inversely proportional to r_c^2 and n, and the value of a_{ij}, defined in (30), is inversely proportional to r_c^4 and n. These observations imply that (i) controlling particles size via n and r_c is clearly more effective than via k_BT; and (ii) increasing r_c results in a faster decrease in the particle size than increasing n.

From this approximate analysis, we can see that there are many possible combinations of n and r_c that reduces a_{eff}. One can employ $r_c = 1$ with a large value of n (fine coarse-graining level with a standard cutoff radius). Or one can employ, for example $n = 3$ with a larger value of $r_c > 1$ (coarser graining limit with a larger cutoff radius). It is noted that the number of interacting pairs is proportional to the cube of the cut-off distance [21].

5 Numerical examples

In this section, we investigate numerically the effects of the number density, cutoff radius and thermodynamic temperature on the solvent particle size as well as on the rheological properties of monodispersed suspensions through 2D simulations. Here, the problem domain is chosen as $L_x \times L_y = 20 \times 20$ and the input parameters employed are $\sigma = 3$, $s = 1/2$, $n = 3 - 9$, $r_c = 1 - 4$ and $k_BT = 0.25 - 1$. To represent the suspended particles, we utilise the spring model using 4-6 basic particles per colloid with $H = 3000$. The rheological properties of suspensions are predicted by conducting the simulation in a simple shear flow. The relative viscosity (suspension/solvent) is calculated in an average sense from ten simulations - each simulation consists of 300,000 time steps. For "zero-shear-rate" viscosity, we compute it at a shear rate of 0.1 for $\phi \leq 0.1$ and 0.01 for $\phi > 0.1$.

The exclusion zone of the particle can be measured by the radial distribution function (RDF) approach

$$g(q) = \frac{1}{N/A} \frac{h}{2\pi q \Delta q}, \tag{39}$$

where A is the area of the domain containing N particles and h is the number of particles in a

circular shell of width $q \to (q + \Delta q)$ at distance q from the centre of the reference particle. If $g(q) = 0$, there is no neighbouring particle at distance q. If $g(q) > 0$, neighbouring particles can be found at the distance q, with a larger value of $g(q)$ indicating more neighbouring particles. In the modelling of the solvent phase, it is desirable to have $g(q) > 0$ (ideally, $g(q) \to 1$ for an infinite number of solvent particles) as the distance q approaches zero.

Figures 5, 6 and 7 show variations of the function $g(q)$ under several given values of the number density n, cutoff radius r_c and temperature k_BT, respectively. The exclusion zones are clearly observed to be smaller as the parameters n and r_c increase, which confirm the trends predicted by our approximate analysis in Section 4. One can thus control the solvent particle size effectively by means of n and r_c. It should be pointed out that an increase in r_c leads to a decrease in the exclusion zone size. Regarding k_BT, the approximate analysis of particle size (Section 4) shows that there are two contributions, one from the conservative force and the other from the dissipative and random force, and their effects are in opposite directions, resulting to a slight effect of k_BT. This is reflected in Figure 4 as reducing k_BT from unity does not make any significant changes in the RDF curve.

We employ the spring model to represent suspended particles (circular discs in 2D). The construction process is as follows. Assume that the solvent particles have a uniform distribution. Average distance between the solvent particles can be estimated as $\bar{d} = (1/d)\sum_{i=1}^{d}(1/n_i)$, where d is the flow dimensionality and n_i is the number density in the i direction ($n = \prod n_i$). Reference sites are placed on the centre of the colloidal particle and uniformly on the surface at a distance $\alpha\bar{d}$ to the centre (Figure 8). Choosing $\alpha < 1$ will help prevent penetration of the solvent particles into the core region of the colloid. Basic DPD particles are then attached to these reference sites via springs. We employ $\alpha = 0.25$ and several sets of reference sites in this study.

5.1 Simulation of suspensions with large number densities

As shown earlier, the DPD system with low number densities (e.g., $n = 3$) and standard values of the other DPD parameters (e.g., $k_BT = 1$, $\sigma = 3$, $r_c = 1$) results in a relatively large exclusion zone and therefore may not be able to represent the solvent phase correctly. Here, we investigate the behaviour of the DPD system as the number density n is increased.

Figure 9 shows exclusion zones of the colloidal particles, which are modelled by a set of 4 basic constituent particles, over a range of solvent density $n = (3, 6, 9)$. Increasing the solvent density also makes the exclusion zone smaller. However, at $n = 9$, one is still able to see clearly a nearly-zero zone around the centre of the particle, which is in contrast to the solvent particle case, where values of the radial distribution function still remain quite large (about 0.35) as the distance approaches zero (Figure 5). As will be shown later, one can easily increase the size of the colloidal particle by just using more its constituent particles.

Figure 10 reveals that the zero-shear-rate relative viscosity curves collapse onto a single curve at large values of the number density. It implies that the size effect of the particles size ratio (colloidal/solvent) becomes negligible at fine coarse graining levels, i.e., at $n \geq 6$. Theoretical estimate for the relative viscosity in the dilute regime [26] is included.

Figure 11 shows a comparison of the present relative viscosities and those predicted by the empirical model of Krieger and Dougherty [27], defined as

$$\eta_r = \left(1 - \frac{\phi}{\phi_m}\right)^{-\phi_m[\eta]} \tag{40}$$

where ϕ_m is the maximal packing fraction and $[\eta]$ the intrinsic viscosity. In 2D, the maximal volume fraction is 0.91 for hexagonal close packing and the intrinsic viscosity is 2 for rigid cylinders. It can be seen that a fine coarse graining level $n = 9$ results in viscosities that are located along the empirical curve of $\phi_m = 0.91$ over the whole range of volume fraction. In contrast, results at a coarser graining level of $n = 3$ fail to follow the correlation; it is in close agreement with the correlation using $\phi_m = 0.76$ up to a semidilute regime, but under-predicts the correlation in the concentrated regime. SPH results [28], where short range lubrication forces are included explicitly, are also shown in the figure. Thus it is seen that the present DPD method at a fine coarse graining level follows the established correlation well.

The size of colloids can be adjusted by means of their constituent particles. Larger sizes will be achieved by simply increasing the number of constituent particles. This can be verified numerically. Figure 12 shows that the constituent particles on a colloid generates a more intensive conservative force field as their number increases. Figure 13 displays larger exclusion zones achieved, measured by radial distribution function, as the number of constituent particles of the colloid increases. It is

expected that, at a fine coarse graining level, a further increase in the colloidal particle size will not affect the relative viscosity curve. This is confirmed in Figure 14 for all regimes: dilute, semidilute and concentrated.

5.2 Simulation of suspensions with large cutoff radii

In this section, we investigate the behaviour of the DPD system as the cutoff radius is increased. The effects of r_c can be seen clearer in the case of using small number densities than in the case of large number densities. Consider the upper coarse graining at $n = 3$. As shown in Figure 6, the solvent particle size is significantly reduced as the cutoff radius r_c increases. The relative viscosity - volume fraction relation for $n = 3$ and $r_c = 2$ is shown in Figure 15. By increasing r_c, a coarse level $n = 3$ is able to produce results following Krieger-Dougherty correlation.

5.3 Simulation of suspensions with low thermodynamic temperature

Unlike the number density n and cutoff radius r_c, reducing the temperature k_BT does not affect the solvent particle size significantly as shown in Figure 7. We now examine effects of k_BT on the colloidal particle size and the results obtained are shown in Figure 16. From these results, it is expected that changing k_BT has little effect on the size ratio of the colloidal to solvent particle, and this is confirmed in Figure 17 for relative viscosity versus volume fraction and also in Figure 18 for relative viscosity versus shear rate (shear thinning behaviour). The effects of k_BT here are in sharp contrast to those in the DPD systems of a variable compressibility reported in [17], where a_{ij} was kept constant, and therefore solvents of different compressibility are compared. For a correct comparison, the solvent compressibility must be kept constant.

6 Concluding remarks

This paper investigates the size effects of solvent particles in the DPD modelling of colloidal suspensions. To better mimic the physical system, the DPD system should be designed to have as small a solvent particle as possible in order to make the colloidal/solvent size ratio as large

as possible (e.g., a few orders of magnitude). The size of DPD particles is found to be decided not only by the conservative force but also by the dissipative and random forces. By keeping the compressibility of the system unchanged, it is shown that the solvent phase can be modelled correctly (in the sense just mentioned above) at both low (large number density) and high (low number density) coarse-graining levels. In the former, one can simply employ standard values of the other input DPD parameters, while in the latter, a larger value of the cutoff radius is required. It is found that the solvent particle size is a decreasing function of the cutoff radius and varying the temperature is not an effective way of controlling the solvent particle size. When the requirement of large colloidal/solvent particles size is met, the DPD results for the reduced viscosity are basically identical for any values of the input DPD parameters.

Acknowledgement

This work is supported by The Agency for Science, Technology and Research (A*STAR) through grant #102 164 0146. N. Mai-Duy also would like to thank the Australian Research Council for an ARC Future Fellowship. We would like to thank the Reviewers for their helpful comments.

References

1. J. Mewis, N.J. Wagner, Colloidal Suspension Rheology, Cambridge University Press, London, 2012.

2. D.R. Foss, J.F. Brady, J. Fluid Mech. 407 (2000) 167.

3. A. Sierou, J.F. Brady, J. Fluid Mech. 448 (2001) 115-146.

4. A.J.C. Ladd, J. Fluid Mech. 271 (1994) 285-309.

5. P.J. Hoogerbrugge, J.M.V.A. Koelman, Europhys. Lett. 19(3) (1992) 155-160.

6. P. Español, M. Revenga, Phys. Rev. E 67(2) (2003) 026705.

7. C. Marsh, Theoretical aspects of dissipative particle dynamics, D.Phil. Thesis, University of Oxford, 1998.

8. N. Phan-Thien, Understanding Viscoelasticity - An Introduction to Rheology, second ed., Springer, Berlin, 2013.

9. W. Dzwinel, D.A. Yuen, J. Colloid Interf. Sci. 225(1) (2000) 179-190.

10. V. Pryamitsyn, V. Ganesan, J. Chem. Phys. 122 (2005) 104906.

11. W. Pan, B. Caswell, G.E. Karniadakis, Langmuir 26(1) (2010) 133-142.

12. M. Whittle, K.P. Travis, J. Chem. Phys. 132 (2010) 124906.

13. N. Mai-Duy, D. Pan, N. Phan-Thien, B.C. Khoo, J. Rheol. 57(2)(2013) 585.

14. J.M.V.A. Koelman, P.J. Hoogerbrugge, Europhys. Lett. 21(3) (1993) 363-368.

15. E.S. Boek, P.V. Coveney, H.N.N. Lekkerkerker, P. van der Schoot, Phys. Rev. E 55(3) (1997) 3124-3133.

16. N.S. Martys, J. Rheol. 49 (2005) 401.

17. N. Phan-Thien, N. Mai-Duy, B.C. Khoo, J. Rheol. 58 (2014) 839.

18. R.M. Füchslin, H. Fellermann, A. Eriksson, H.-J. Ziock, J. Chem. Phys. 130 (2009) 214102.

19. P. Español, P. Warren, Europhys. Lett. 30(4) (1995) 191-196.

20. R.D. Groot, P.B. Warren, J. Chem. Phys. 107 (1997) 4423.

21. X. Fan, N. Phan-Thien, S. Chen, X. Wu, T.Y. Ng, Phys. Fluids 18(6) (2006) 063102.

22. P. Español, Phys. Rev. E 52 (1995) 1734-1742.

23. J.H. Irving, J.G. Kirkwood, J. Chem. Phys. 18 (1950) 817.

24. D. Pan, N. Phan-Thien, N. Mai-Duy, B.C. Khoo, J. Comput. Phys. 242 (2013) 196-210.

25. C.A. Marsh, G. Backx, M.H. Ernst, Phys. Rev. E 56(2) (1997) 1676-1691.

26. J.F. Brady, Int. J. Multiphas. Flow 10(1) (1984) 113-114.

27. I.M. Krieger, T.J. Dougherty, Trans. Soc. Rheol. 3 (1959) 137.

28. X. Bian, M. Ellero, Comput. Phys. Commun. 85(1) (2014) 53-62.

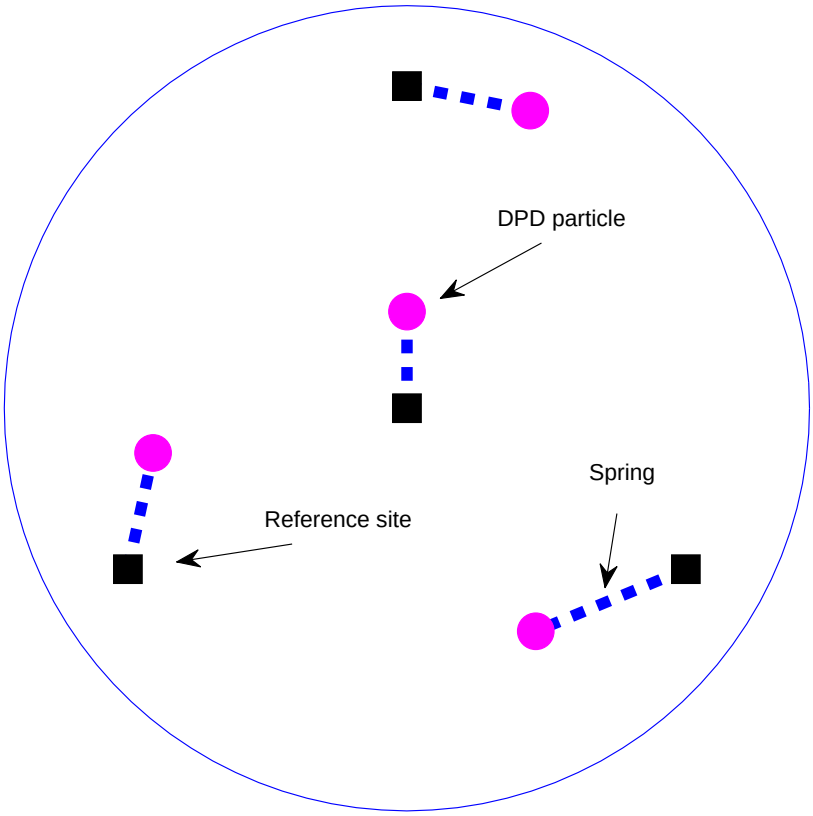

Figure 1: Schematic diagram of the spring model. A colloidal particle is modelled by a small set of basic DPD particles connected to reference sites through linear springs of very large stiffness. The reference sites, collectively modeling a rigid body, move as a rigid body motion calculated through their Newton-Euler equations.

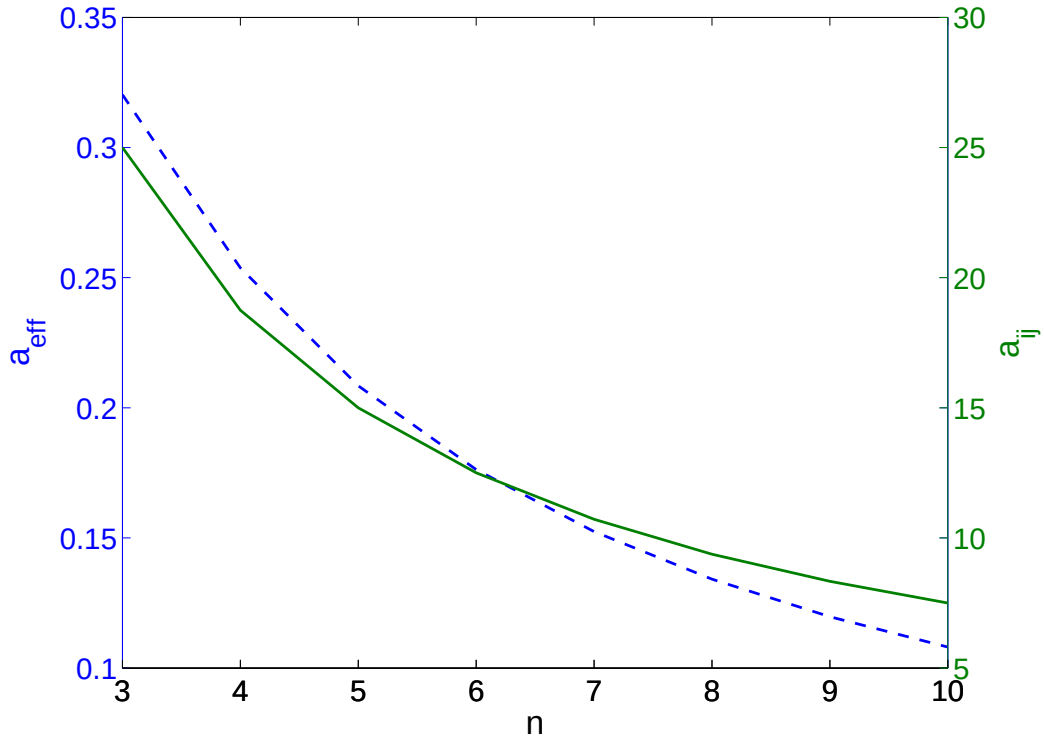

Figure 2: DPD system, $m = 1$, $k_B T = 1$, $r_c = 1$: effects of the number density on the particle size (the dash line representing the zone size caused by the dissipative and random forces (Eqn. (38)) and the solid line by the conservative force (Eqn. (30))).

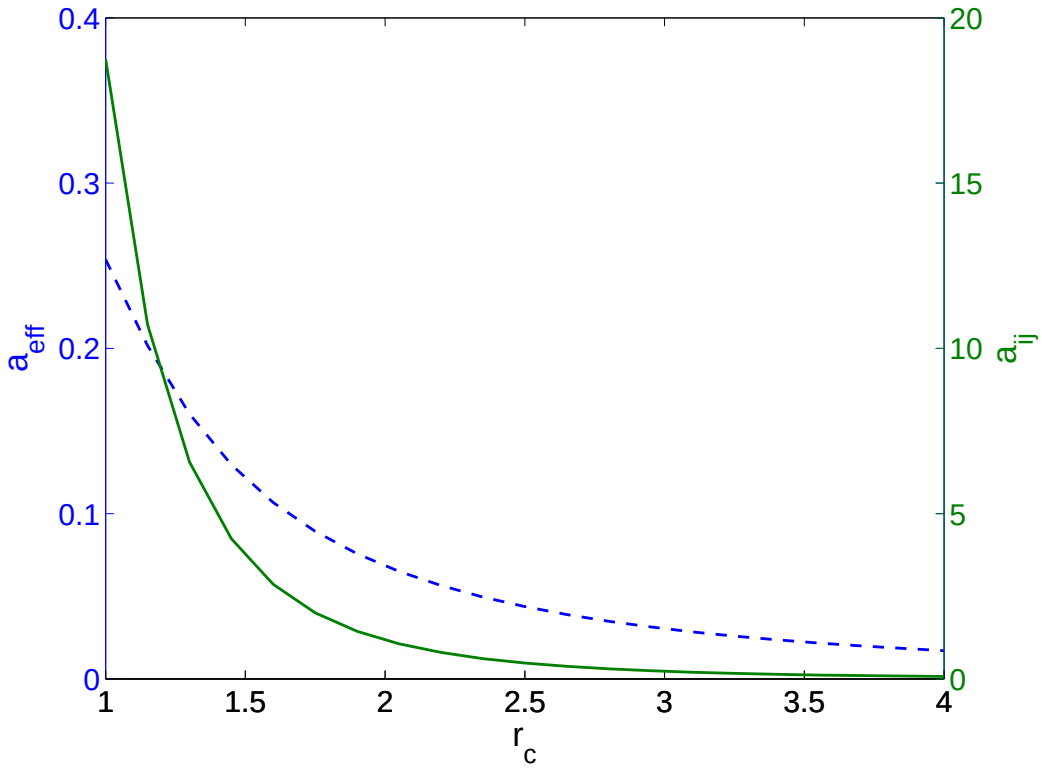

Figure 3: DPD system, $m = 1$, $k_BT = 1$, $n = 4$: effects of the cutoff radius on the particle size (the dash line representing the zone size caused by the dissipative and random forces (Eqn. (38)) and the solid line by the conservative force (Eqn. (30))).

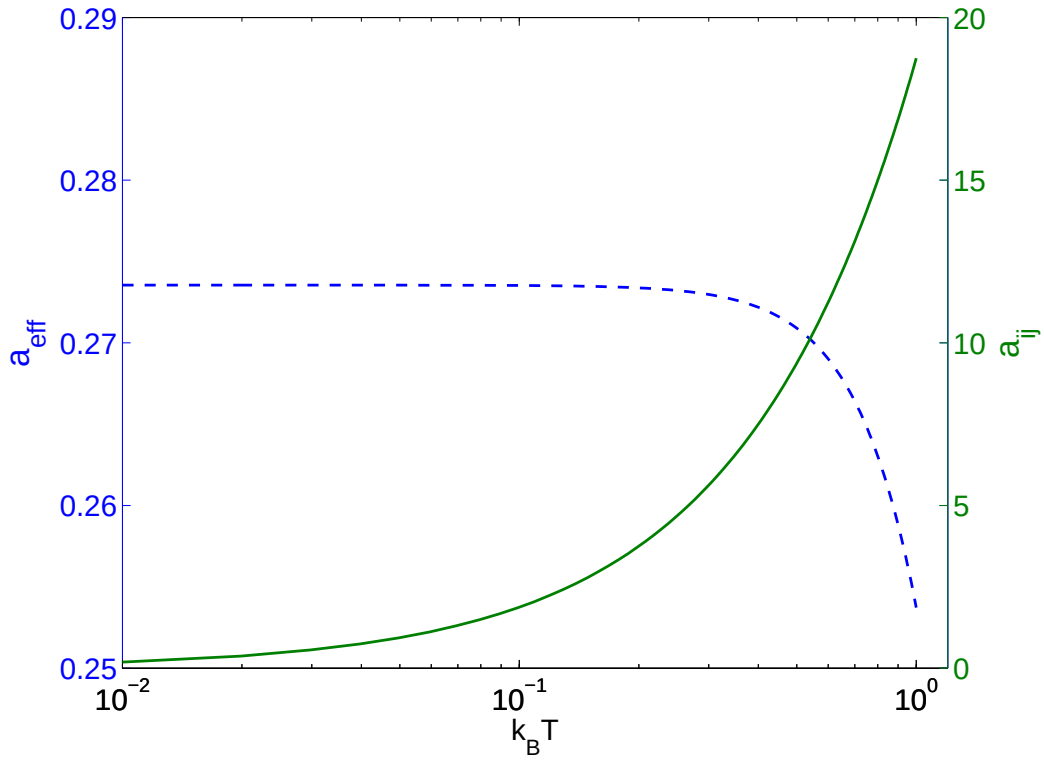

Figure 4: DPD system, $m = 1$, $n = 4$, $r_c = 1$: effects of the thermodynamic temperature on the particle size (the dash line representing the zone size caused by the dissipative and random forces (Eqn. (38)) and the solid line by the conservative force (Eqn. (30))).

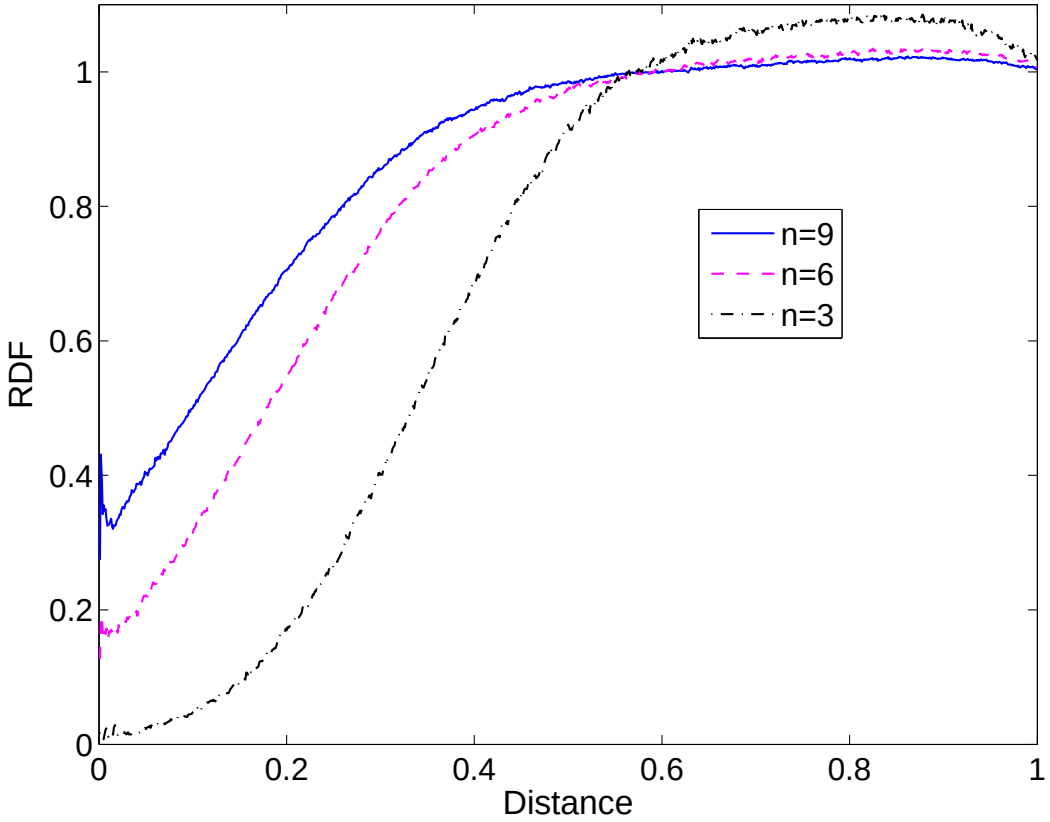

Figure 5: DPD system, $r_c = 1$, $k_B T = 1$, $L_x \times L_y = 20 \times 20$, $\Delta t = 0.001$, $\Delta q = 0.001$: Exclusion zone of the solvent particle is effectively reduced in size as the number density increases. Note that the physical properties of the system, temperature and compressibility, are kept constant.

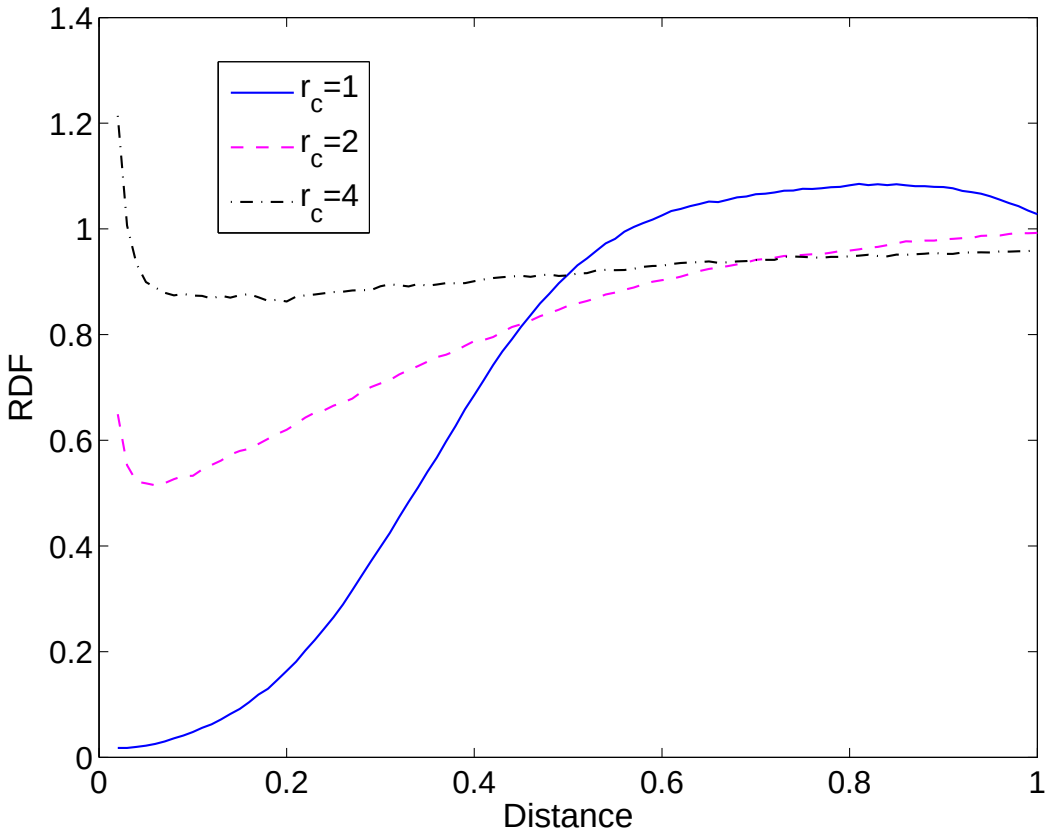

Figure 6: DPD system, $n = 3$, $k_BT = 1$, $L_x \times L_y = 20 \times 20$, $\Delta t = 0.001$, $\Delta q = 0.01$: Exclusion zone of the solvent particle is effectively reduced in size as the cut-off radius increases. Note that the physical properties of the system, temperature and compressibility, are kept constant.

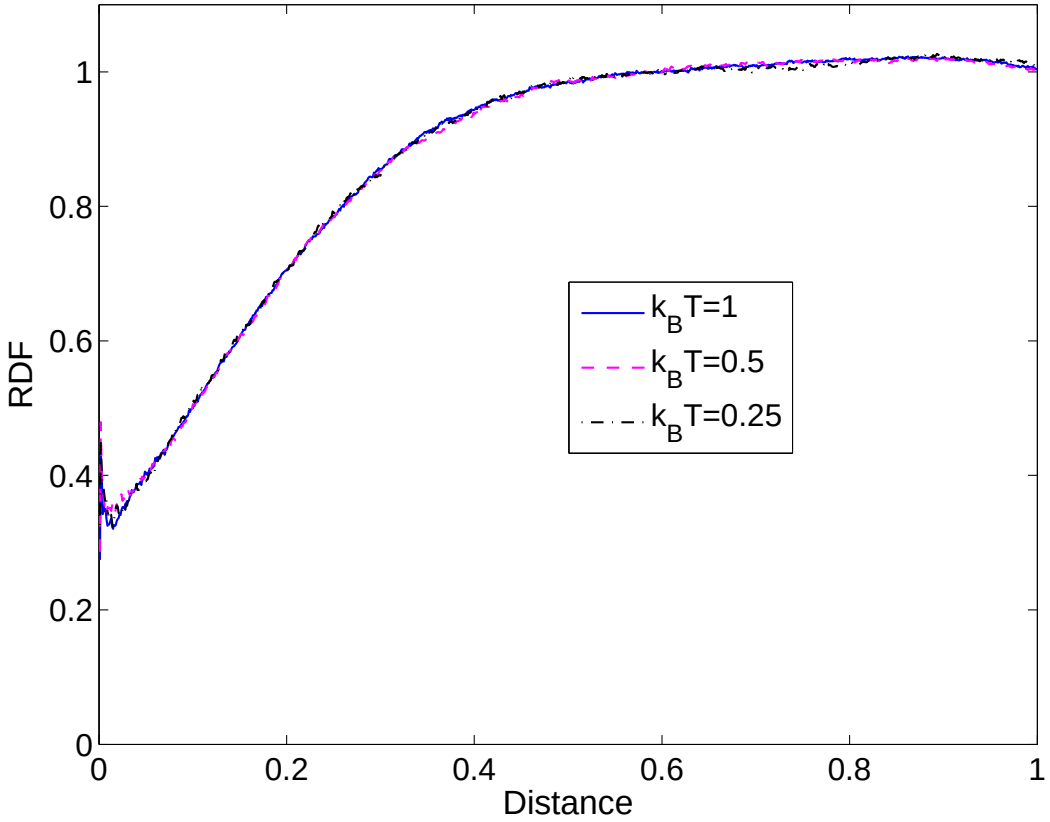

Figure 7: DPD system, $r_c = 1$, $n = 9$, $L_x \times L_y = 20 \times 20$, $\Delta t = 0.001$, $\Delta q = 0.001$: reducing the thermodynamic temperature does not affect the RDF results of the solvent particle. Note that the physical property of compressibility of the system is kept constant.

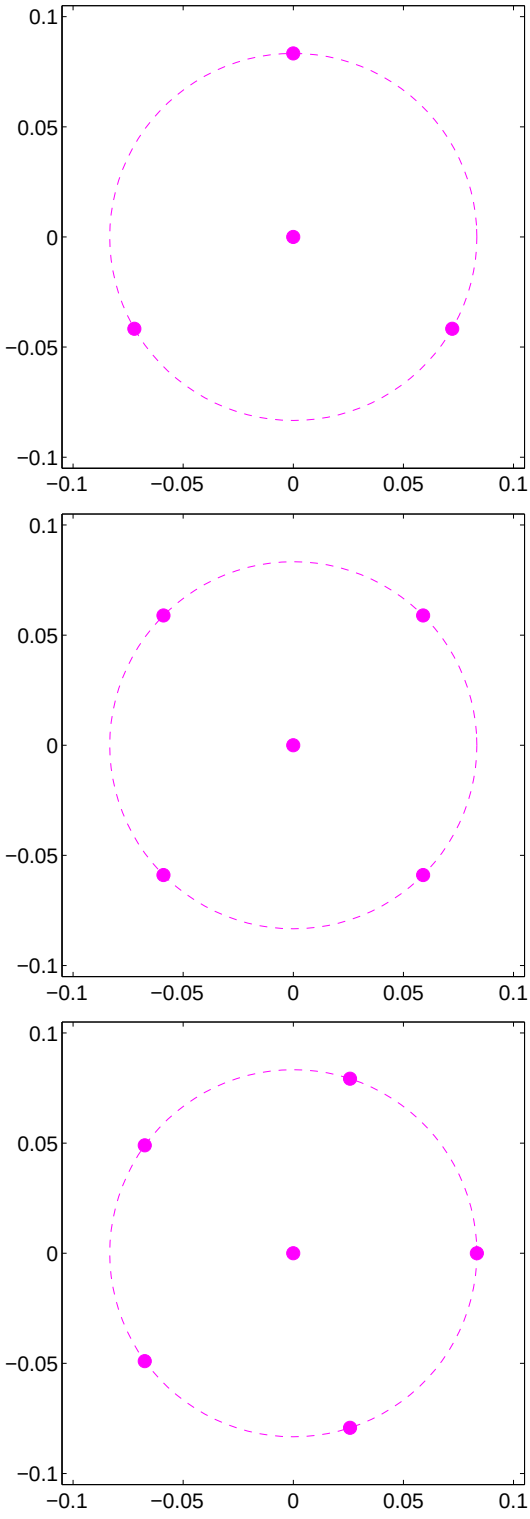

Figure 8: Colloidal circular discs are modelled with different numbers of constituent particles. The radius r is computed as $0.25\bar{d}$ in which n is the number density of the solvent particles and $\bar{d}$ the average distance between the solvent particles. Here, $n = 9$ leads to $r = 0.0833$.

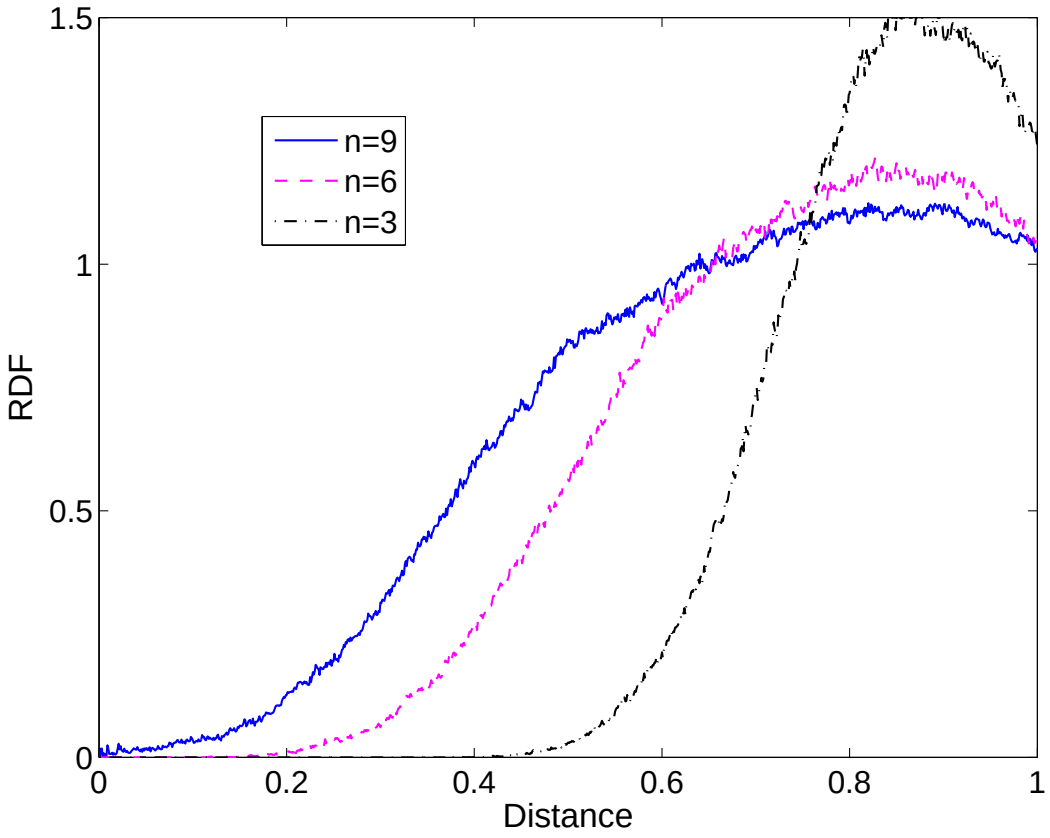

Figure 9: Suspension, $r_c = 1$, $k_BT = 1$, $L_x \times L_y = 20 \times 20$, $\Delta t = 0.001$, $\Delta q = 0.001$: Exclusion zone of the colloidal particle is also reduced as the number density increases. It is noted that the colloidal particle is constructed using a set of 4 basic DPD particles.

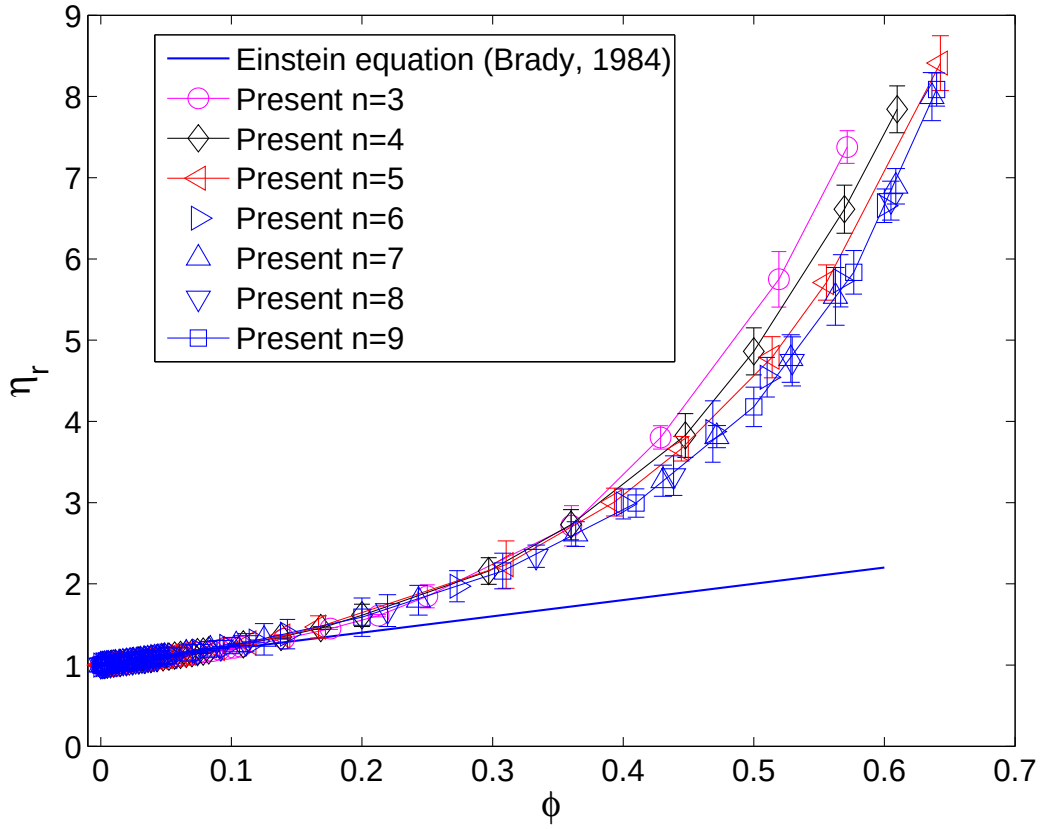

Figure 10: Suspension, $k_BT = 1$, $r_c = 1$, 4 basic DPD particles per colloid, $L_x \times L_y = 20 \times 20$: the computed relative viscosity curves collapse onto a single curve at large values of the number density of the solvent particles. Theoretical estimation for dilute regime [Brady (1984)] is included.

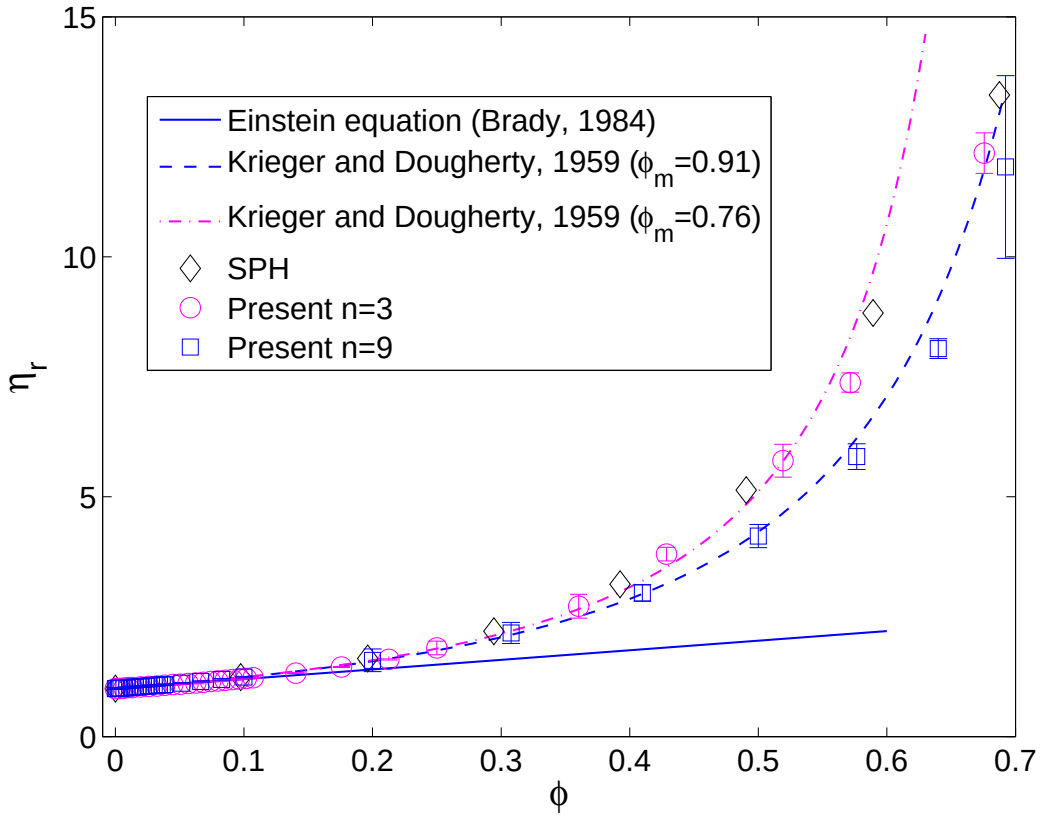

Figure 11: Suspension, $k_BT = 1$, $r_c = 1$, 4 basic DPD particles per colloid, $L_x \times L_y = 20 \times 20$: Results by a fine coarse graining level ($n = 9$) can follow the Krieger and Dougherty curve of $\phi_m = 0.91$, while the upper coarse graining limit $n = 3$ fails to do so for the curve of $\phi_m = 0.76$. Note that SPH results, where short-range lubrication forces are taken into account explicitly, are included and their behaviour is similar to that of the case $n = 3$.

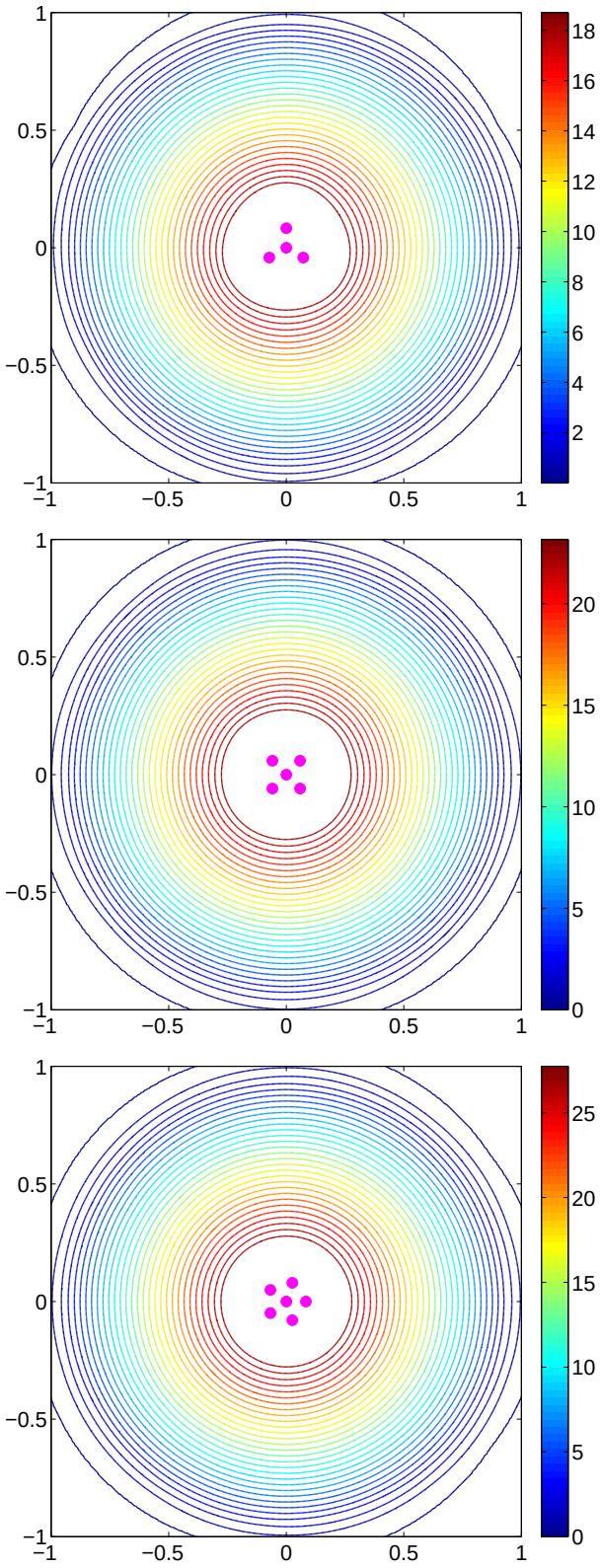

Figure 12: 2D circular discs, $n = 9$: several configurations of the colloidal particle and their conservative force fields. Values of the total conservative force at $r = 0.25$ are 18.7044, 23.1648 and 27.7394 for 4, 5 and 6 constituent particles, respectively. The force field thus becomes greater as the number of constituent particles increases.

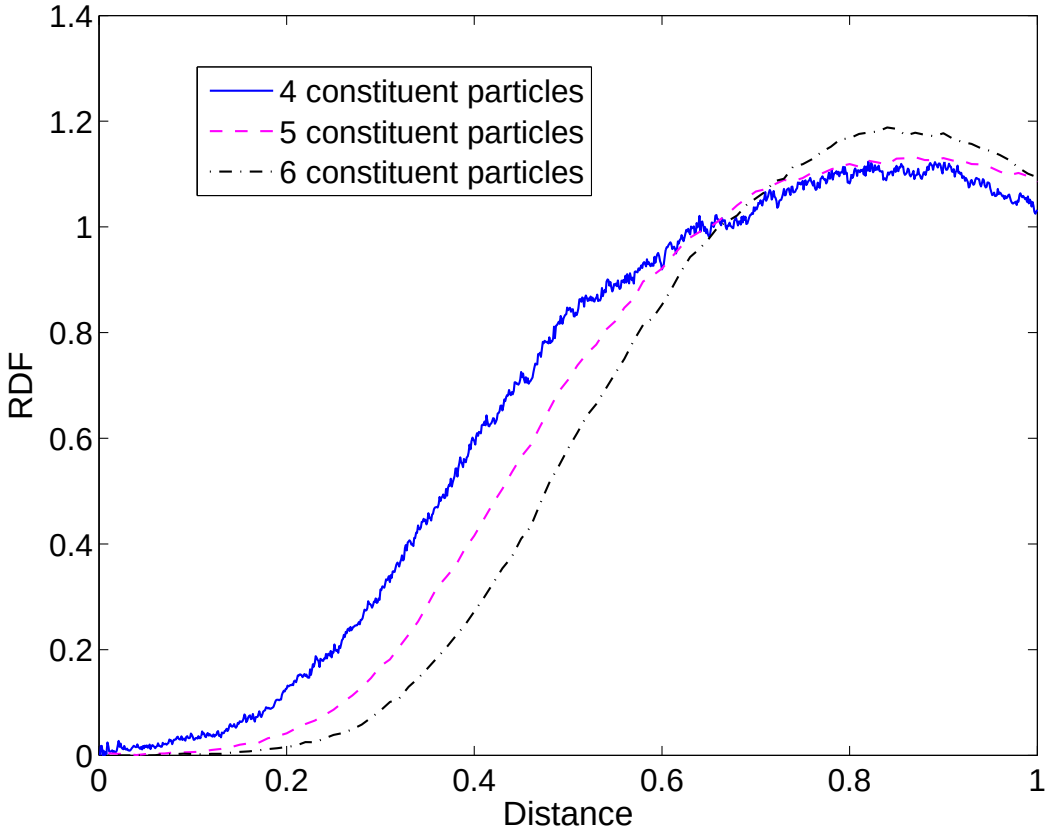

Figure 13: Suspension, $n = 9$, $L_x \times L_y = 20 \times 20$, $\Delta t = 0.01$, $\Delta q = 0.01$: radial distribution functions of 3 types of suspended particles that are formed by 4, 5 and 6 constituent particles. The size of exclusive zone is seen to be larger as the number of constituent particles increases.

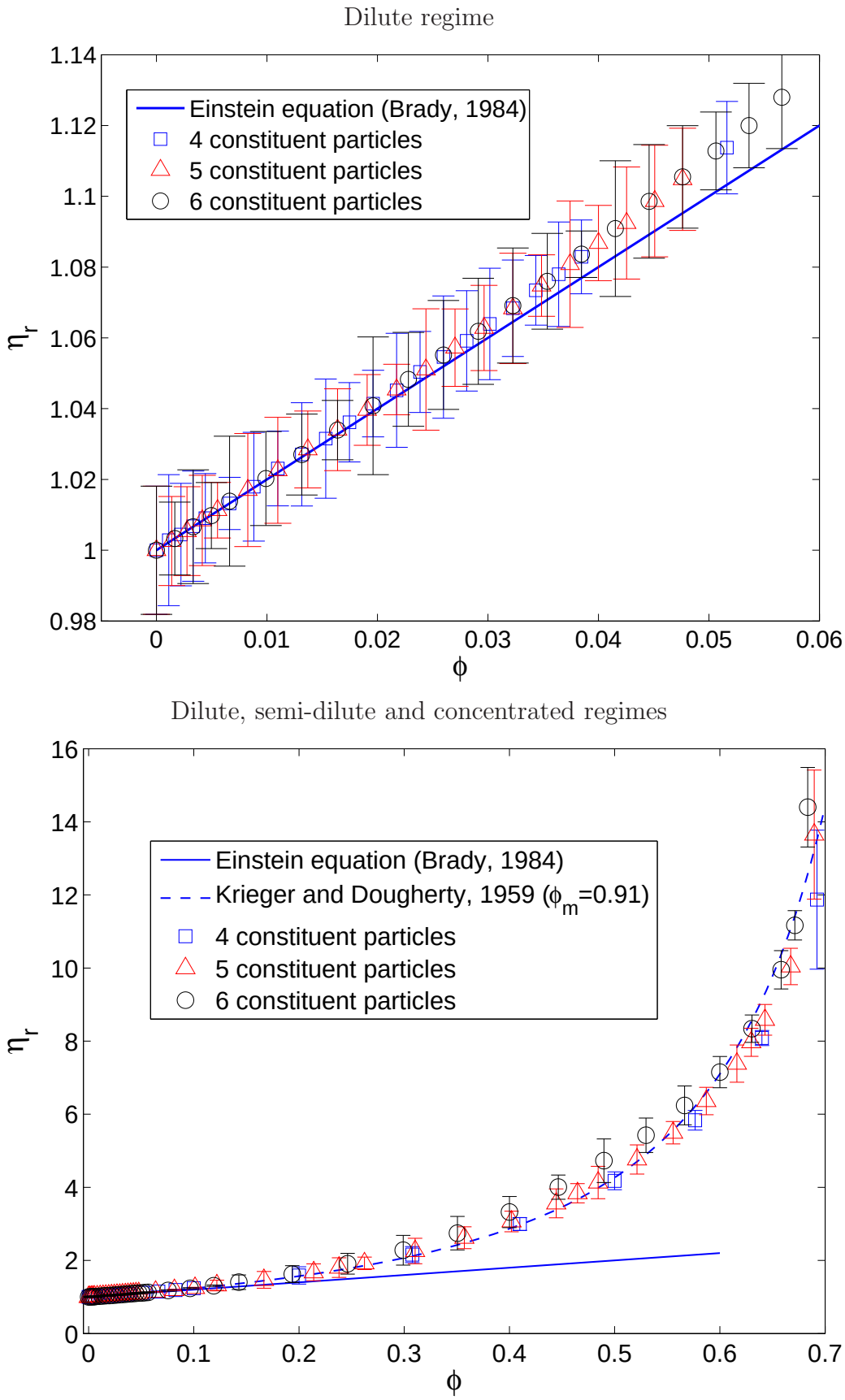

Figure 14: Suspension, $n = 9$, $r_c = 1$, $L_x \times L_y = 20 \times 20$, $\Delta t = 0.01$: similar relative viscosities are obtained with colloids of different configurations: 4, 5 and 6 basic particles packed into a colloid. Note that the corresponding numbers of colloids used are in the range of 1 to 2025, 1 to 1600 and 1 to 1296, respectively.

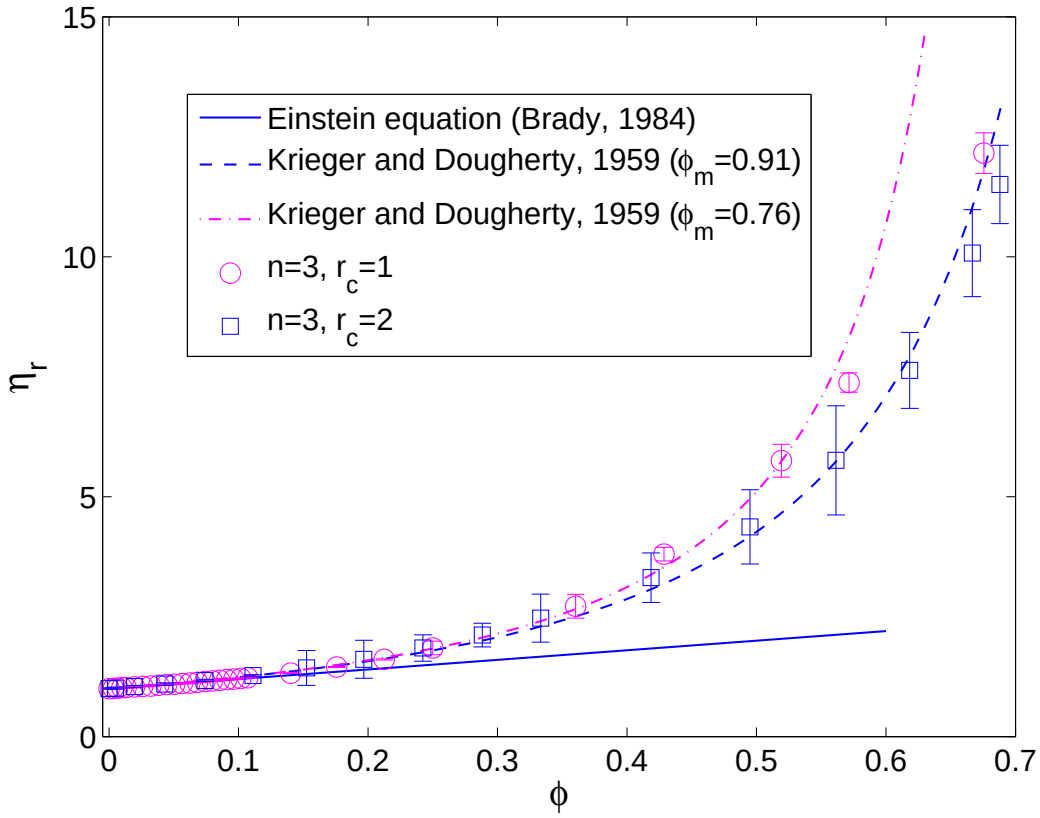

Figure 15: Suspension, $k_BT = 1$, $L_x \times L_y = 20 \times 20$: Effects of solvent particle size in upper coarse-graining limit ($n = 3$, 6 constituent particles per colloid) are significantly reduced as the cutoff radius r_c increases. Increasing r_c will enhance the dissipative/hydrodynamic contribution (viscous interaction, liquid regime) in the DPD system and smaller time steps are thus needed to prevent the system temperature departing from the specified value (here, $k_BT = 1$). We employ $\Delta t = 0.01$ for $r_c = 1$ and $\Delta t = 0.005$ for $r_c = 2$. Note that the solvent viscosity is 1.8935 for $r_c = 1$, but up to 25.2018 for $r_c = 2$.

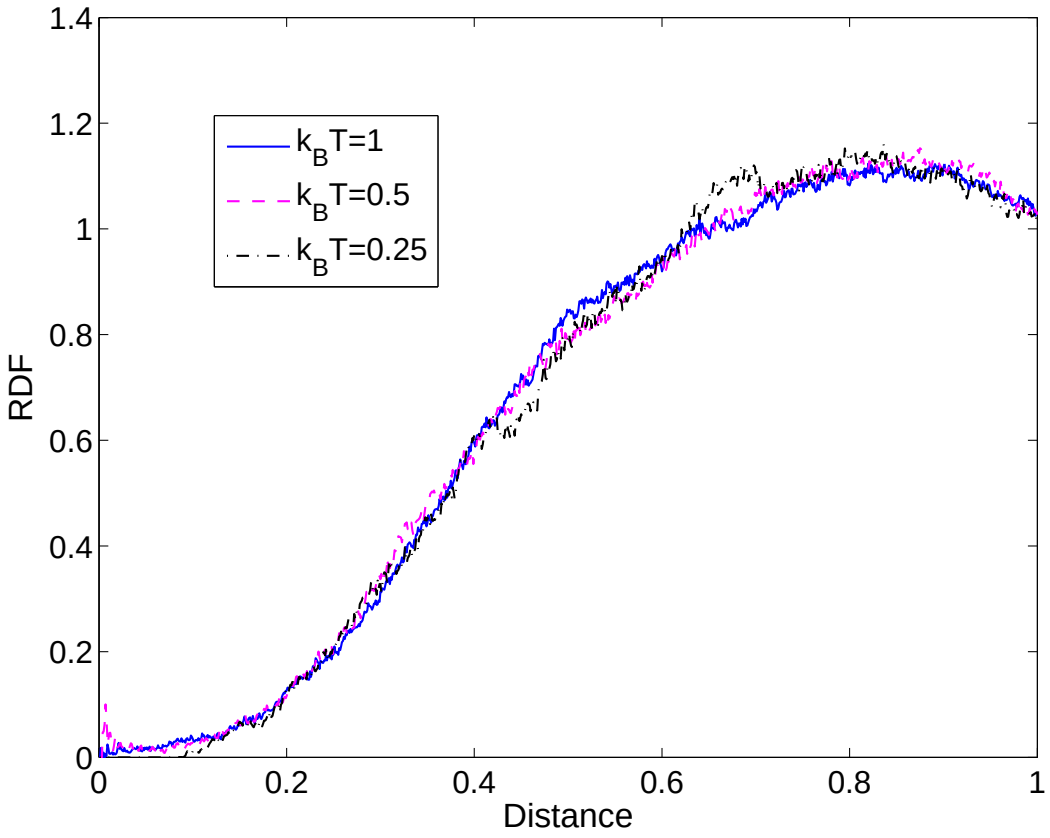

Figure 16: Suspension, $r_c = 1$, $n = 9$, $L_x \times L_y = 20 \times 20$, $\Delta t = 0.001$, $\Delta q = 0.001$: reducing $k_B T$ does not affect the RDF results of the colloidal particle. It is noted that the colloid is constructed using a set of 4 basic DPD particles.

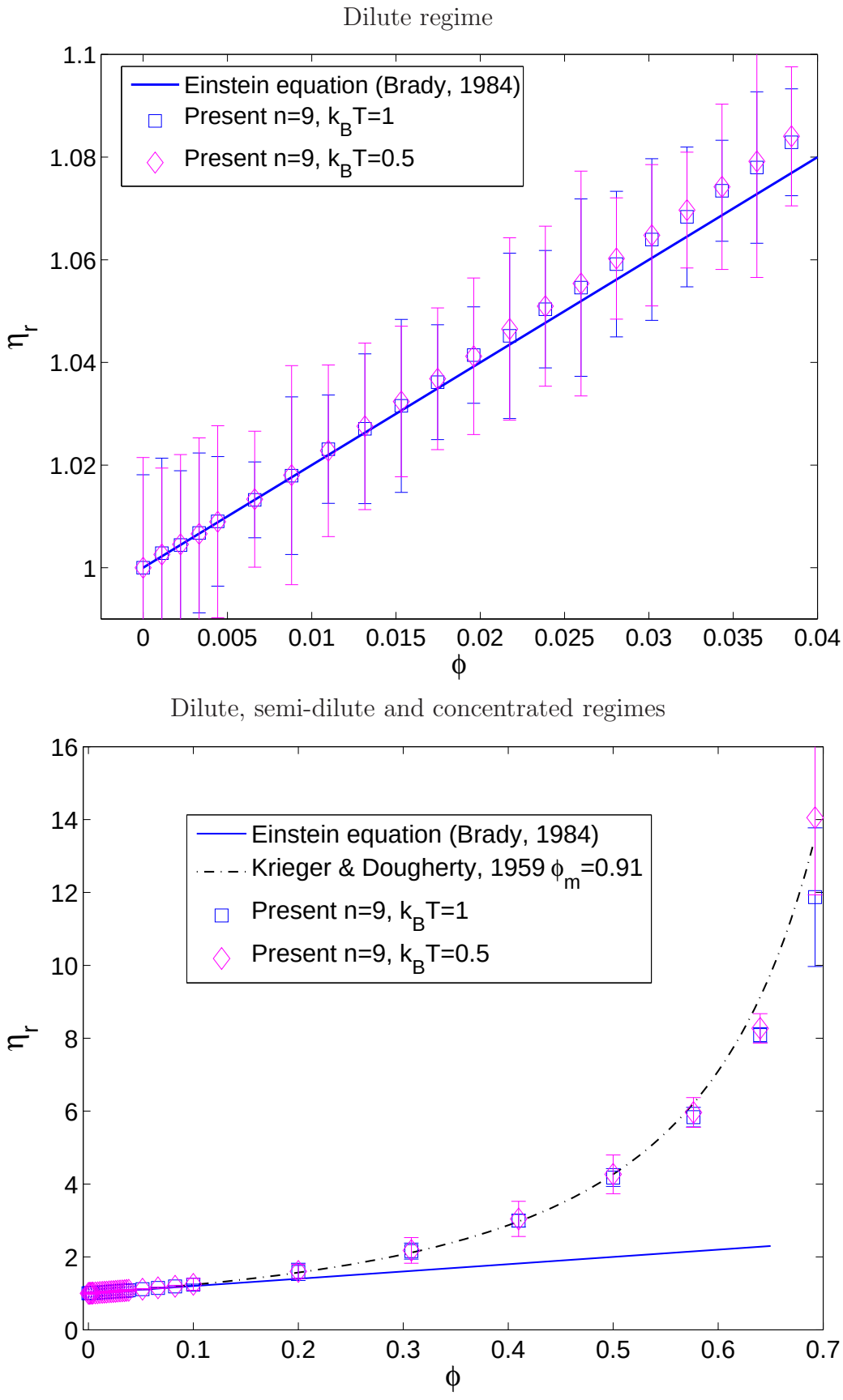

Figure 17: Suspension, $n = 9$, $r_c = 1$, $L_x \times L_y = 20 \times 20$: similar relative viscosities are obtained with different values of k_BT. Note that we employ $\Delta t = 0.01$ for $k_BT = 1$ and $\Delta t = 0.005$ for $k_BT = 0.5$.

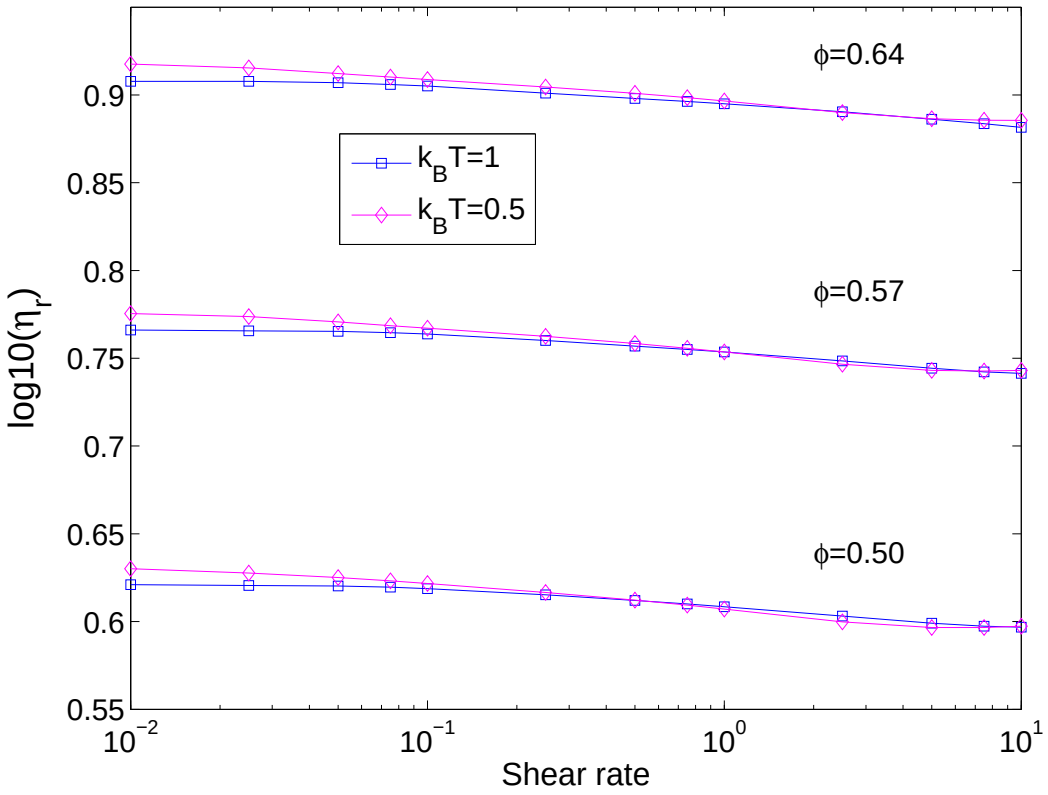

Figure 18: 2D suspensions, $n = 9$, $r_c = 1$, $L_x \times L_y = 20 \times 20$: Two cases of k_BT have similar shear thinning behaviour. Unlike the case of variable compressibility [17], the effect of the thermodynamic temperature on the degree of shear-thinning can be negligible here. Note that we employ $\Delta t = 0.01$ for $k_BT = 1$ and $\Delta t = 0.005$ for $k_BT = 0.5$.